hsa_circ_0004846 enhances the malignant phenotype of papillary thyroid carcinoma cells via the miR-142-3p/PELI1 axis

XIAOJIE DING[1,2], RUIQI LI[1], JINGYA XU[1], GUANGQUAN HU[3], WENPING WANG[2], QIHUAN LV[4] and YOUMIN WANG[1]

[1]Department of Endocrinology, The First Affiliated Hospital of Anhui Medical University, Hefei, Anhui 230022, P.R. China; [2]Department of Endocrinology, Anhui No. 2 Provincial People's Hospital, Hefei, Anhui 230041, P.R. China; [3]Department of Cardiology, The Second Affiliated Hospital of Anhui Medical University, Hefei, Anhui 230601, P.R. China; [4]Department of International Medical Service, The First Affiliated Hospital of University of Science and Technology of China, Hefei, Anhui 230001, P.R. China

Received September 24, 2024; Accepted January 28, 2025

DOI: 10.3892/ol.2025.14949

Abstract. Circular RNAs (circRNAs) are closely associated with human tumorigenesis; however, whether hsa_circ_0004846 serves a role in the progression of papillary thyroid carcinoma (PTC) remains unclear. Therefore, the present study aimed to investigate the effect of hsa_circ_0004846 on PTC. The results demonstrated that circ_0004846 was abnormally upregulated in PTC tissues and thyroid cancer cell lines (BCPAP, TPC-1 and IHH-4). Furthermore, hsa_circ_0004846-overexpressing or -depleted PTC cell lines (TPC-1 and IHH-4) were constructed using a lentiviral vector system. Notably, hsa_circ_0004846 overexpression markedly promoted cell proliferation, migration and invasion, as evidenced by activation of the PI3K/AKT pathway and the upregulation of vimentin, a class-III intermediate filament, which acts by regulating cell attachment and migration. However, hsa_circ_0004846 knockdown displayed the opposite effects. Mechanistically, the regulatory association among hsa_circ_0004846, microRNA (miR)-142-3p and Pellino E3 ubiquitin protein ligase 1 (PELI1) was validated using a dual-luciferase reporter assay. Specifically, the results demonstrated that hsa_circ_0004846 could sponge miR-142-3p, and the expression levels of miR-142-3p were negatively associated with those of hsa_circ_0004846. In addition, PELI1, a cancer-related E3 ubiquitin ligase, was identified as a downstream target of the hsa_circ_0004846/miR-142-3p axis in PTC. Therefore, PELI1 silencing could reverse the hsa_circ_0004846-induced malignant phenotype of PTC cells. Taken together, the results of the current study highlighted the effect of the hsa_circ_0004846/miR-142-3p/PELI1 regulatory network on PTC progression, thus providing a promising target for PTC treatment.

Correspondence to: Dr Youmin Wang, Department of Endocrinology, The First Affiliated Hospital of Anhui Medical University, 218 Jixi Road, Hefei, Anhui 230022, P.R. China
E-mail: wangym19640810@163.com

Key words: hsa_circ_0004846, microRNA-142-3p, Pellino E3 ubiquitin protein ligase 1, papillary thyroid carcinoma

Introduction

Papillary thyroid carcinoma (PTC) is the most common pathological subtype of thyroid cancer, followed by follicular and medullary thyroid cancer (1). Due to its increasing incidence rate, PTC is considered a serious concern for society (2). Although the majority of PTC cases have a relatively good prognosis, the risk of regional recurrence and PTC-related deaths should not be underestimated in patients with lymph node infiltration (3,4). Unlike medullary thyroid cancer, which is characterized by the secretion of calcitonin and carcinoembryonic antigen, there are no significant molecular biomarkers for PTC (1). Therefore, more research on the identification of novel biomarkers is needed for the early diagnosis and individual treatment of patients with PTC.

Circular RNAs (circRNAs) are a class of endogenous non-coding RNAs, which are usually generated by the back-cleavage of exons in protein-encoding genes (5). Due to their tissue-specific expression profile and highly conserved characteristics, circRNAs have become targets for cancer treatment (6,7). Zhang *et al* (8) revealed that circ_TIAM1 may be involved in the development of PTC by acting as an oncogene. Additionally, another study demonstrated that circ_102171 could interact with CTNNBIP1 protein to activate the Wnt/β-catenin pathway, thus promoting PTC progression (9). However, the role and mechanism of circRNAs in PTC remain to be elucidated.

hsa_circ_0004846, also known as circ_SAMD4A (chr14: 55168779-55169298), is a circRNA with a length of 519 nucleotides that is derived from the reverse cleavage of SAMD4A mRNA. Previous studies have shown that hsa_circ_0004846 is involved in the development of osteosarcoma (10,11). For example, Zhao *et al* (11) revealed that hsa_circ_0004846 could enhance the proliferation and the stemness features of osteosarcoma cells. Furthermore, hsa_circ_0004846 silencing has been shown to suppress the epithelial-mesenchymal transition and malignant behavior of osteosarcoma cells (12). However,

to the best of our knowledge, there are currently no reports on the role of hsa_circ_0004846 in other types of cancer, including PTC.

With the advancement of sequencing technology, circRNAs have been shown to regulate the expression of their target genes by acting as competing endogenous RNAs (ceRNAs) of microRNAs (miRNAs/miRs) (13). miRNAs, a class of endogenous and small noncoding RNAs, act as regulators of cell-cell communication during tumor progression (14). For example, miR-221 and miR-222 have been reported to be significantly upregulated in PTC compared with in benign thyroid nodules (15). Emerging evidence has suggested that serum miRNAs, such as miR-146-b and miR-221, may be considered as novel biomarkers for diagnosing PTC (16). Furthermore, miR-142-3p may induce apoptosis, and inhibit cell proliferation and metastasis in PTC (17). However, the regulatory mechanism of miR-142-3p in PTC remains unclear.

The present study aimed to reveal the role of hsa_circ_0004846 in PTC. Therefore, hsa_circ_0004846-overexpressing and -depleted TPC-1 and IHH-4 cell lines were established. Based on the ceRNA hypothesis, the current study further explored whether the effect of hsa_circ_0004846 on PTC cells was mediated by the miR-142-3p/Pellino E3 ubiquitin protein ligase 1 (PELI1) axis.

Materials and methods

Human tissue samples. A total of 34 pairs of frozen PTC tissues and paracancerous tissues were obtained from patients (mean age, 45 years; age range, 20-65 years; 7 male patients and 27 female patients) who underwent surgical resection at The First Affiliated Hospital of Anhui Medical University (Hefei, China) between February 2021 and June 2022. No patients received radiotherapy or chemotherapy before surgery, and there was no history of neck radiation exposure during adolescence or childhood.

Cell culture. The thyroid cancer cell line BCPAP, the PTC cell line TPC-1 and the normal human thyroid cell line Nthy-ori 3-1 were purchased from iCell Bioscience Inc., and were cultured in RPMI-1640 medium (Beijing Solarbio Science & Technology Co., Ltd.) supplemented with 10% fetal bovine serum (FBS; Zhejiang Tianhang Biotechnology Co., Ltd.). Another PTC cell line (IHH-4) was obtained from Nanjing CoBioer Biotechnology Co., Ltd. and was maintained in DMEM (Wuhan Servicebio Technology Co., Ltd.) supplemented with 10% FBS, penicillin (100 U/ml) and streptomycin (100 mg/ml). All cells were incubated at 37˚C in an incubator containing 5% CO_2. Profiling and authentication of BCPAP, TPC-1, IHH-4 and Nthy-ori 3-1 cell lines was performed using the short tandem repeat identification criteria developed by the International Cell Line Authentication Committee (18).

Cell transduction and transfection. The EGFP-expressing lentivirus vector pLKO.1-EGFP-puro was purchased from Hunan Fenghui Biotechnology Co., Ltd. (cat. no. FH1717), whereas the GFP-expressing pLC5-ciR lentivirus vector was obtained from Guangzhou Geneseed Biotech Co., Ltd. The short hairpin RNA (shRNA) against hsa_circ_0004846 (sh-circRNA; sense, 5'-CAAGAATCATTAACCAATGGC-3' and antisense, 5'-GCCATTGGTTAATGATTCTTG-3') and the corresponding negative control shRNA (sh-NC; sense, 5'-TTCTCCGAACGTGTCACGT-3' and antisense, 5'-ACG TGACACGTTCGGAGAA-3') were obtained from General Biology (Anhui) Co., Ltd., and were sub-cloned into the pLKO.1-EGFP-puro lentivirus vector. The full-length hsa_circ_0004846 sequence was sub-cloned into the pLC5-ciR lentivirus vector (Lv-circRNA). The empty pLC5-ciR was used as a negative control (Lv-Vector).

To obtain lentiviral particles, the 2nd lentiviral generation system was used. Briefly, 293T cells (Cellverse Co., Ltd.) were transfected with 14 μg lentiviral plasmids, 10.5 μg packaging plasmids and 3.5 μg envelope plasmids using Lipofectamine™ 3000 (Invitrogen; Thermo Fisher Scientific, Inc.) for 6 h at 37˚C. After replacing the medium with fresh medium, the lentiviral particles were collected after continued incubation for 72 h at 37˚C. For stable transduction, the aforementioned lentivirus particles (Lv-sh-NC, Lv-sh-circRNA, Lv-Vector and Lv-circRNA) were used to infect TPC-1 (MOI=10) and IHH-4 (MOI=20) cells. After 24 h, TPC-1 cells were selected with 2 μg/ml puromycin and IHH-4 cells were selected with 3 μg/ml puromycin for 7 days. The maintenance concentration of puromycin used for TPC-1 and IHH-4 cells was 1 and 1.5 μg/ml, respectively. Subsequently, a BX53 fluorescence microscope (Olympus Corporation) was used to confirm the transduction efficiency. Once the stably transduced cells were constructed, the cells underwent subsequent experiments according to the experimental protocol.

miR-142-3p-mimic, NC-mimic, PELI1 small interfering (si)RNA (si-PEL1) and the siRNA negative control (si-NC) were purchased from General Biology (Anhui) Co., Ltd. The sequences were as follows: miR-142-3p-mimic sense, 5'-UGU AGUGUUUCCUACUUUAUGGA-3', antisense, 5'-UCCAUA AAGUAGGAAACACUACA-3'; NC-mimic sense, 5'-UUC UCCGAACGUGUCACGUTT-3', antisense, 5'-ACGUGACAC GUUCGGAGAATT-3'; si-PELI1 sense, 5'-CAGUCAGUA CAAAGCACUAUATT-3', antisense, UAUAGUGCUUUG UACUGACUGTT; and si-NC sense, 5'-UUCUCCGAACGU GUCACGUTT-3', antisense, 5'-ACGUGACACGUUCGG AGAATT-3'. TPC-1 cells were transfected with the indicated mimics (75 pmol) and siRNAs (75 pmol) using Lipofectamine 3000 for 15 min at 37˚C. according to the manufacturer's protocol. A total of 48 h after transfection, the cells were collected for subsequent experiments.

Reverse transcription-quantitative PCR (RT-qPCR). Total RNA was extracted from cells and tissues using the TRIpure Reagent (BioTeke Corporation), and was then reverse transcribed into the corresponding cDNA using the BeyoRT II M-MLV reverse transcriptase (Beyotime Institute of Biotechnology) or the miRNA First Strand cDNA Synthesis (Tailing Reaction) Kit (cat. no. B532451; Sangon Biotech Co., Ltd.) according to the manufacturers' protocols. qPCR was performed on the Exicycler™ 96 system (Bioneer Corporation) using SYBR Green (Beijing Solarbio Science & Technology Co., Ltd.) and 2X Taq PCR MasterMix kit (Beijing Solarbio Science & Technology Co., Ltd.). The cycling conditions comprised an initial denaturation step for 5 min at 95˚C, followed by 40 cycles at 95˚C for 10 sec (denaturation), annealing at 60˚C for 10 sec and elongation at 72˚C for 15 sec.

The expression levels of the target mRNA and circRNA were normalized to the housekeeping gene β-actin, whereas miR-142-3p expression was normalized to U6. The relative quantification of target genes in frozen clinical PTC/paracancerous tissues and cultured cells was calculated using the $2^{-\Delta Cq}$ and $2^{-\Delta\Delta Cq}$ methods, respectively (19). The primer sequences were as follows: hsa_circ_0004846 forward, 5'-CGGGATTCT GGGATTTG-3'; reverse, 5'-TTGGGCAGCAGTTTCAT-3'; PELI1 forward, 5'-CTACCGTGAAGCATTTA-3'; reverse, 5'-ACAGAGGAACATAGGGA-3'; β-actin forward, 5'-GGC ACCCAGCACAATGAA-3'; reverse, 5'-TAGAAGCATTTG CGGTGG-3'; and miR-142-3p forward, 5'-TGTAGTGTTTCC TACTTTATGGA-3'. The U6 primers and the miR-142-3p reverse primer were contained in the corresponding miRNA First Strand cDNA Synthesis (Tailing Reaction) kit for RT.

Characterization of hsa_circ_0004846. Total RNA was extracted from TPC-1 cells using the TRIpure Reagent, and was then reverse transcribed into the corresponding cDNA using the BeyoRT II M-MLV reverse transcriptase according to manufacturer's protocol. Genomic DNA (gDNA) was extracted from TPC-1 cells by using a gDNA extraction kit (BioTeke Corporation). To validate the formation of hsa_circ_0004846, the divergent primer (DP) sequences that amplify only circular transcripts and the convergent primer (CP) sequences that detect linear RNA molecules were designed to amplify linear mRNA (SAMD4A; Fig. 1A) and hsa_circ_0004846 using cDNA and gDNA as templates. β-actin was employed as the internal control. The sequences of the primers were as follows: hsa_circ_0004846 CP (forward, 5'-GGGATTCTGGGATTTGC-3'; reverse, 5'-CGTATTGAT TGTGGTGGG-3'); hsa_circ_0004846 DP (forward, 5'-CGG GATTCTGGGATTTG-3'; reverse, 5'-TTGGGCAGCAGT TTCAT-3'); β-actin CP (forward, 5'-GGCACCCAGCAC AATGAA-3'; reverse, 5'-TAGAAGCATTTGCGGTGG-3'); and the DP for β-actin (forward, 5'-GCCTCGCTGTCCACC TT-3'; reverse, 5'-TCTGACCCATGCCCACC-3'), which was used as a negative control. Semi-quantitative PCR was carried out on the Exicycler™ 96 machine (Bioneer Corporation) in a 20-μl reaction system containing 1 μl cDNA or gDNA, 10 μl 2X Taq PCR MasterMix and 1 μl forward/reverse primer for divergent primers (DPs) and convergent primers (CPs), respectively. The thermocycling condition were as follows: 2 min at 94˚C for pre-denaturation; 40 cycles at 94˚C for 10 sec for denaturation, 54˚C for 20 sec for annealing and 72˚C for 30 sec for extension. β-actin was used as a loading control. Subsequently, 1.5% agarose gel (Biowest) was used for electrophoresis of PCR products, and Gold View dye (Beijing Solarbio Science & Technology Co., Ltd.) was used for visualization.

Western blot analysis. Total protein extracts were isolated from cells using the RIPA lysis buffer (Beijing Solarbio Science & Technology Co., Ltd.) and were quantified using the BCA Protein Assay Kit (Beijing Solarbio Science & Technology Co., Ltd.). Western blot analysis was performed as previously described (12). The primary antibodies used were as follows: Anti-phosphorylated (p)-AKT (cat. no. AP0140; dilution, 1:500), anti-AKT (cat. no. A17909; dilution, 1:1,000), anti-p-glycogen synthase kinase-3β (GSK-3β; cat. no. AP0039; dilution, 1:500) and anti-GSK-3β (cat. no. A2081; dilution, 1:1,000) (all from ABclonal Biotech Co., Ltd). The following secondary antibodies were purchased from Beijing Solarbio Science & Technology Co., Ltd.: Goat anti-rabbit IgG/HRP (cat. no. SE134; dilution, 1:3,000) and goat anti-mouse IgG/HRP (cat. no. SE131; dilution, 1:3,000). GAPDH (cat. no. 60004-1-Ig; dilution, 1:20,000; Wuhan Sanying Biotechnology) was used as the internal control.

Cell Counting Kit 8 (CCK-8) assay. Cell proliferation and viability were assessed using a CCK-8 Assay Kit (Nanjing KeyGen Biotech Co., Ltd.), according to the manufacturer's instructions. Briefly, after being transfected for 48 h, $5x10^3$ cells/well were seeded into 96-well plates and incubated for 24, 48 or 72 h. Subsequently, each well was supplemented with 10 μl CCK-8 solution and incubated for an additional 2 h. Finally, the absorbance in each well was measured at a wavelength of 450 nm using an 800TS Microplate Reader (Biotek; Agilent Technologies, Inc.).

Colony formation assay. The colony formation assay was performed as previously described (20). Briefly, TPC-1 and IHH-4 cells transduced with the corresponding lentiviral particles were seeded into culture dishes (400 cells/dish) and maintained in an incubator for 14 days. After washing with PBS, cells were fixed with 4% paraformaldehyde for 1 min at room temperature and then stained with Wright-Giemsa solution (Nanjing Jiancheng Bioengineering Institute) for 5 min at room temperature. The visible colonies containing ≥50 cells were manually counted under an IX53 light microscope (Olympus Corporation). The colony formation rate was calculated using the following formula: Colony formation rate (%)=(number of colonies/400) x100.

5-ethynyl-2'-deoxyuridine (EdU) staining. The EdU Imaging Detection Kit (Nanjing KeyGen Biotech Co., Ltd.) was utilized to evaluate cell proliferation, according to the manufacturer's instructions. Briefly, transduced TPC-1 and IHH-4 cells were treated with 10 μM EdU staining solution at 37˚C for 2 h, followed by fixing with 4% paraformaldehyde for 15 min at room temperature and staining with the Click-iT reaction solution for 30 min at room temperature. The cell nuclei were stained with DAPI for 5 min at room temperature. Finally, images of the cells were captured under an IX53 light microscope (Olympus Corporation).

Immunofluorescence (IF) staining of vimentin. To detect the protein expression levels of vimentin in PTC cells, IF staining was conducted. Specifically, TPC-1 and IHH-4 cells were fixed with 4% paraformaldehyde for 15 min at room temperature. After washing with PBS, cells were permeabilized with 0.1% Triton X-100 (Beyotime Institute of Biotechnology) for 30 min at room temperature. Subsequently, the slides were blocked with 1% bovine serum albumin (Sangon Biotech Co., Ltd.) for 15 min at room temperature and incubated with a primary antibody against vimentin (cat. no. A19607; dilution, 1:100; ABclonal Biotech Co., Ltd) overnight at 4˚C, followed by incubation with Goat anti-Rabbit IgG (Heavy chain) Superclonal™ Secondary Antibody, Alexa Fluor™ 555 (cat. no. A27039; dilution, 1:200; Invitrogen; Thermo Fisher Scientific, Inc.) for

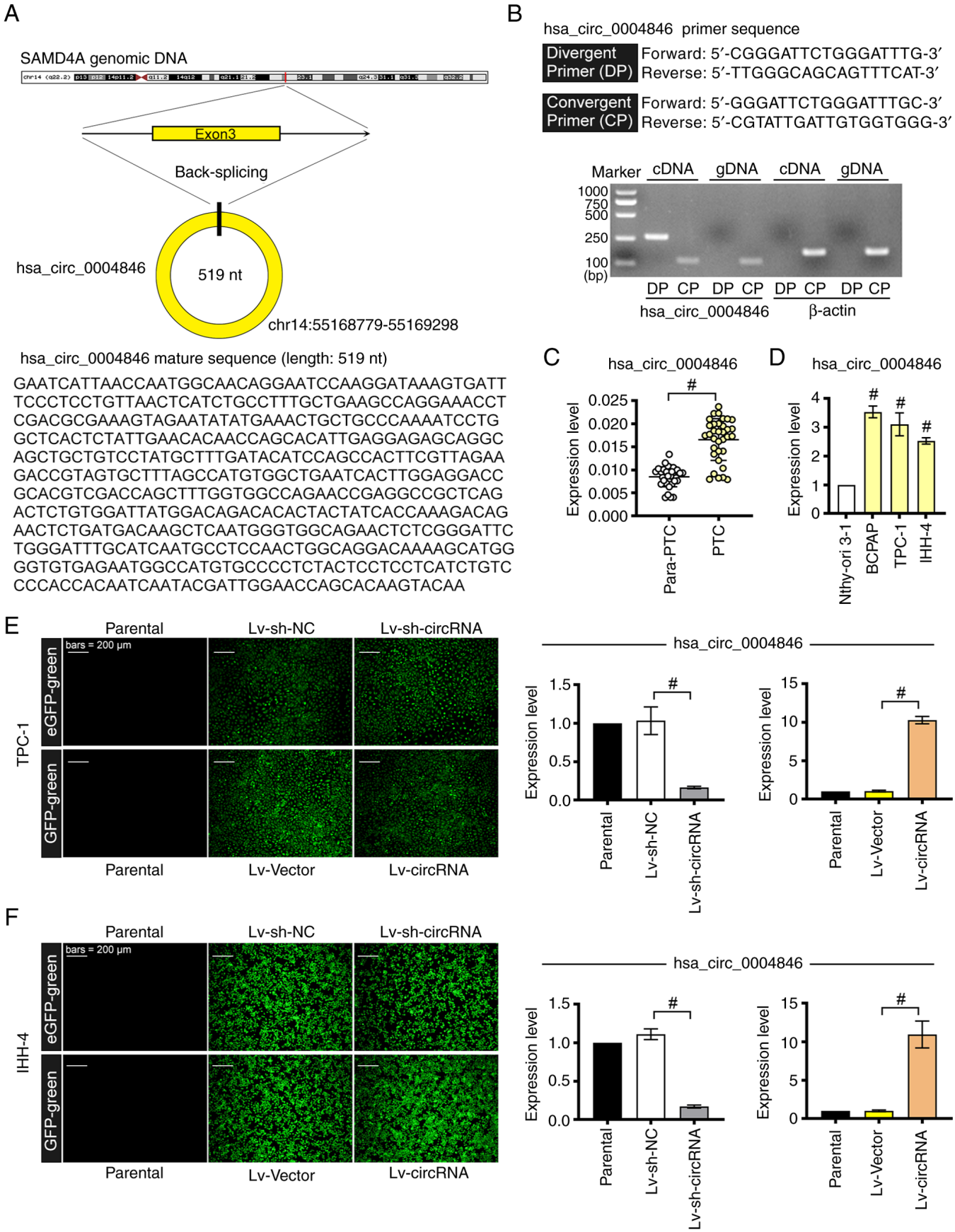

Figure 1. hsa_circ_0004846 is upregulated in PTC. (A) Schematic diagram of the circularization of hsa_circ_0004846. (B) Divergent primers and convergent primers were used to amplify hsa_circ_0004846 in cDNA and gDNA. (C) RT-qPCR detection of hsa_circ_0004846 in 34 PTC tissues and adjacent non-tumor tissues. (D) Expression levels of hsa_circ_0004846 in normal human thyroid cells (Nthy-ori 3-1) and thyroid cancer cells (BCPAP, TPC-1 and IHH-4). Fluorescence images of hsa_circ_0004846-overexpressing or hsa_circ_0004846-depleted (E) TPC-1 and (F) IHH-4 PTC cells. The expression levels of hsa_circ_0004846 were detected by RT-qPCR. $^{\#}P<0.05$. circ, circular; Lv, lentivirus; NC, negative control; PTC, papillary thyroid carcinoma; RT-qPCR, reverse transcription-quantitative PCR; sh, short hairpin.

1 h at room temperature. Subsequently, the cell nuclei were stained with DAPI for 5 min at room temperature and images were captured at magnification of x400 under a BX53 fluorescence microscope (Olympus Corporation).

Cell migration and invasion assays. For the cell migration assay, 300 μl cell suspension containing 5x10^3 PTC cells was added to the upper Transwell chambers (24 wells; pore size, 8.0 μm). For the cell invasion assay, 5x10^4 PTC cells in 300 μl were added to the upper chambers, which were precoated with Matrigel for 2 h at 37˚C. The lower chamber was supplemented with 700 μl culture medium containing 10% FBS. Subsequently, the chambers were incubated in a 37˚C incubator with 5% CO_2. Following incubation for 24 h, the Transwell chambers were washed with PBS, fixed in 4% paraformaldehyde for 20 min at room temperature and stained with 0.5% crystal violet solution (Amresco, LLC) for 5 min at room temperature. Images of the migratory and invasive cells were captured under a light microscope (IX53; Olympus Corporation).

Dual-luciferase reporter assay. For the dual-luciferase reporter assay, the wild-type (WT) and mutant (Mut) sequences of the 3'untranslated region (3'UTR) of PELI1 (WT-PELI1 3'UTR or Mut-PELI1 3'UTR), and WT-hsa_circ_0004846 and Mut-hsa_circ_0004846 fragments were sub-cloned into the pmirGLO vector [General Biology (Anhui) Co., Ltd.]. 293T cells were co-transfected with pmirGLO vectors (pmirGLO-WT-PELI1-3'UTR, pmirGLO-Mut-PELI1-3'UTR, pmirGLO-WT-hsa_circ_0004846 or pmirGLO-hsa_circ_0004846) and miRNA mimics (miR-142-3p-mimic or NC-mimic) using Lipofectamine 3000. After 48 h, firefly and *Renilla* luciferase activities were detected using a dual-luciferase reporter gene assay kit (Nanjing KeyGen Biotech Co., Ltd.). The relative luciferase activity was normalized to *Renilla* luciferase activity.

Bioinformatics analysis. The circRNA Interactome database (https://circinteractome.nia.nih.gov/) was used to predict the downstream targets for hsa_circ_0004846, while an online target prediction (http://www.mirdb.org/) was performed to discover the downstream targets for miR-142-3p.

Statistical analysis. Data are presented as the mean ± SD. The *in vitro* experiments were repeated at last three times. Statistical analysis was performed using GraphPad Prism 9.0 software (Dotmatics). The paired Student's t-test was used to assess the differences between the paired PTC tumor and paracancerous tissues. Unless otherwise specified, the differences between two groups were compared by unpaired Student's t-test (two-tailed), while those among multiple groups were compared using one-way ANOVA followed by Tukey's post hoc test. $P<0.05$ was considered to indicate a statistically significant difference.

Results

hsa_circ_0004846 is upregulated in PTC tissues and thyroid cancer cell lines. hsa_circ_0004846 (length, 519 nucleotides; chr14: 55168779-55169298) is derived from back-splicing of SAMD4A mRNA (Fig. 1A). Firstly, the specificity of the primers for hsa_circ_0004846 were verified by RT-qPCR. As shown in Fig. 1B, convergent primers amplified both cDNA and gDNA, whereas divergent primers detected hsa_circ_0004846 in cDNA but not in gDNA. Subsequently, the analysis revealed that hsa_circ_0004846 was more highly expressed in PTC tissues compared with that in paracancerous tissues (Fig. 1C). Consistently, hsa_circ_0004846 was also upregulated in the thyroid cancer cell line BCPAP and the two PTC cell lines, TPC-1 and IHH-4, compared with that in the Nthy-ori 3-1 normal human thyroid cell line (Fig. 1D). These findings encouraged further investigation of the role of hsa_circ_0004846 in PTC. Therefore, hsa_circ_0004846-overexpressing (Lv-circRNA) and -depleted (Lv-sh-circRNA) TPC-1 and IHH-4 cell lines were established via lentiviral infection. The transduction efficiency was confirmed by fluorescence detection and RT-qPCR analysis (Fig. 1E and F).

hsa_circ_0004846 promotes PTC cell proliferation, migration and invasion. As shown in Fig. 2A and B, TPC-1 and IHH-4 cell proliferation was significantly enhanced following hsa_circ_0004846 overexpression; however, proliferation was markedly reduced in hsa_circ_0004846-depleted PTC cells. Similar results were observed using the colony formation assay (Fig. 2C and D). EdU staining further verified that hsa_circ_0004846 overexpression enhanced PTC cell proliferation, whereas hsa_circ_0004846 knockdown mitigated this process (Fig. 2E and F). Furthermore, Transwell assays showed that hsa_circ_0004846 knockdown significantly attenuated PTC cell migration and invasion (Fig. 3A and B); however, TPC-1 and IHH-4 cells transduced with the hsa_circ_0004846 overexpression lentivirus displayed stronger migratory and invasive capabilities (Fig. 3C and D). Consistently, as shown in Fig. 3E, vimentin loss was observed in hsa_circ_0004846-silenced cells, whereas hsa_circ_0004846-overexpressing cells displayed the opposite effect.

hsa_circ_0004846 activates the PI3K/AKT pathway in PTC cells. Given that the PI3K/AKT pathway serves a notable role in the pathogenesis of PTC (21), the current study further explored whether hsa_circ_0004846-induced PTC cell proliferation was mediated by activation of the PI3K/AKT pathway. As shown in Fig. 4A and B, hsa_circ_0004846 overexpression in TPC-1 and IHH-4 cells upregulated p-AKT and p-GSK-3β. By contrast, hsa_circ_0004846 knockdown notably suppressed the expression levels of p-AKT and p-GSK-3β. However, hsa_circ_0004846 overexpression or silencing had no effect on the protein expression levels of total AKT and GSK-3β.

hsa_circ_0004846 serves as a sponge for miR-142-3p, which in turn targets PELI1 in PTC cells. Bioinformatics analysis was performed using the circRNA Interactome database. The analysis predicted that hsa_circ_0004846 could bind to miR-142-3p (Fig. 5A-a). Dual-luciferase reporter assays verified that the luciferase activity was significantly decreased in cells co-transfected with miR-142-3p-mimic and WT-circRNA compared with that in the NC-mimic + WT-circRNA group (Fig. 5A-b). Furthermore, RT-qPCR analysis indicated that hsa_circ_0004846 knockdown

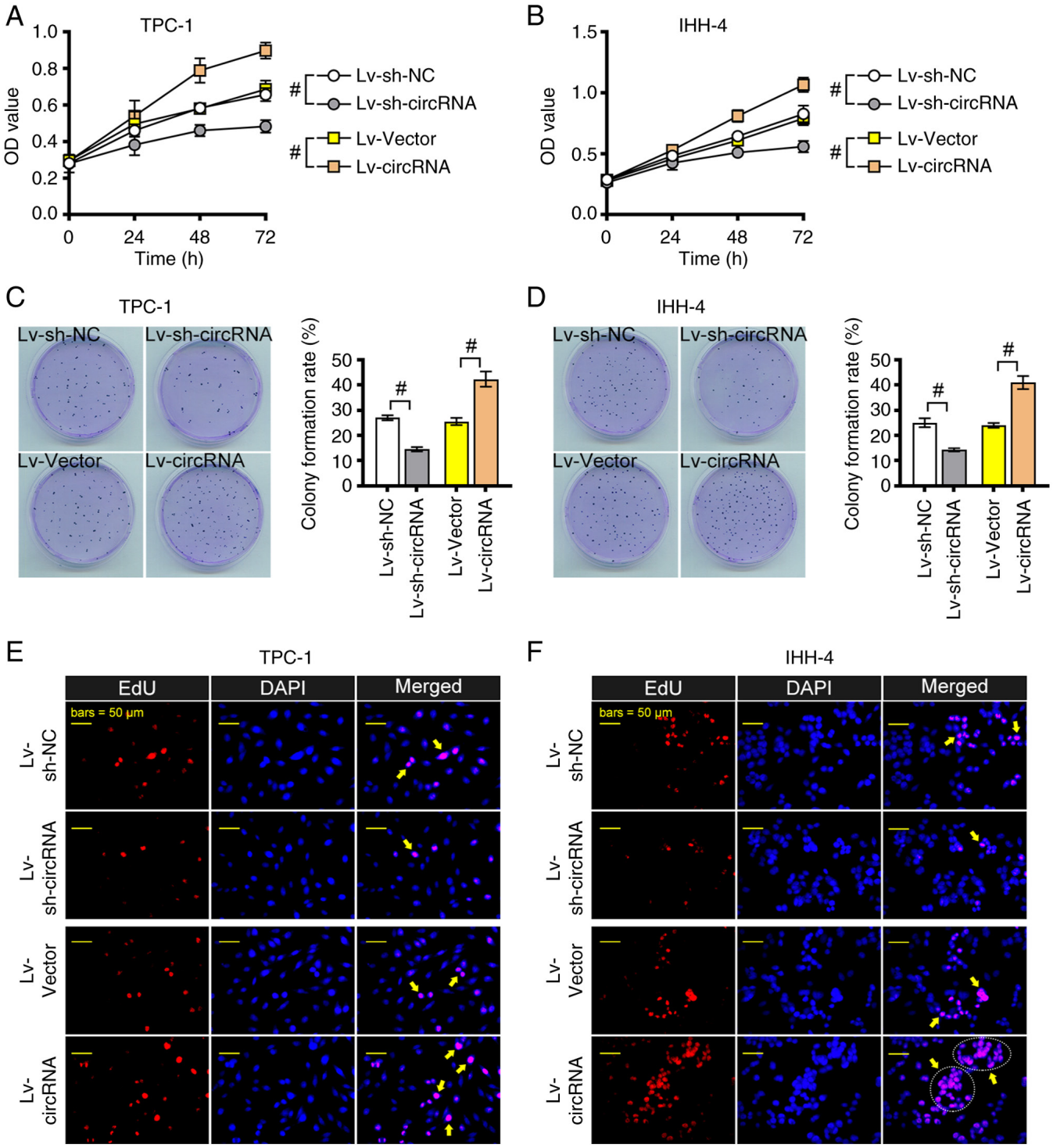

Figure 2. hsa_circ_0004846 promotes PTC cell proliferation. Proliferation of hsa_circ_0004846-depleted or -overexpressing (A) TPC-1 and (B) IHH-4 cells was assessed using the Cell Counting Kit 8 assay. (C and D) Colony formation assays and (E and F) EdU staining were performed to evaluate the effects of hsa_circ_0004846 overexpression or knockdown on PTC cell proliferation. #P<0.05. circ, circular; EdU, 5-ethynyl-2'-deoxyuridine; Lv, lentivirus; NC, negative control; PTC, papillary thyroid carcinoma; sh, short hairpin.

could upregulate miR-142-3p and downregulate PELI1 in TPC-1 cells (Fig. 5B and C). By contrast, downregulated miR-142-3p and upregulated PELI1 expression were observed in hsa_circ_0004846-overexpressing cells. In addition, bioinformatics analysis using an online target prediction suggested that PELI1 could be a downstream target for miR-142-3p (Fig. 5D-a). Dual-luciferase reporter assays verified that co-transfection of cells with WT-PELI1-3'UTR and miR-142-3p-mimic inhibited luciferase activity compared with that in the corresponding control group (WT-PELI1-3'UTR + NC-mimic) (Fig. 5D-b). No significant changes were observed between the Mut-PELI1-3'UTR + miR-142-3p-mimic and Mut-PELI1-3'UTR + NC-mimic groups. Furthermore, TPC-1 cells were transfected with miR-142-3p mimics to overexpress miR-142-3p (Fig. 5E). The subsequent RT-qPCR analysis showed that miR-142-3p

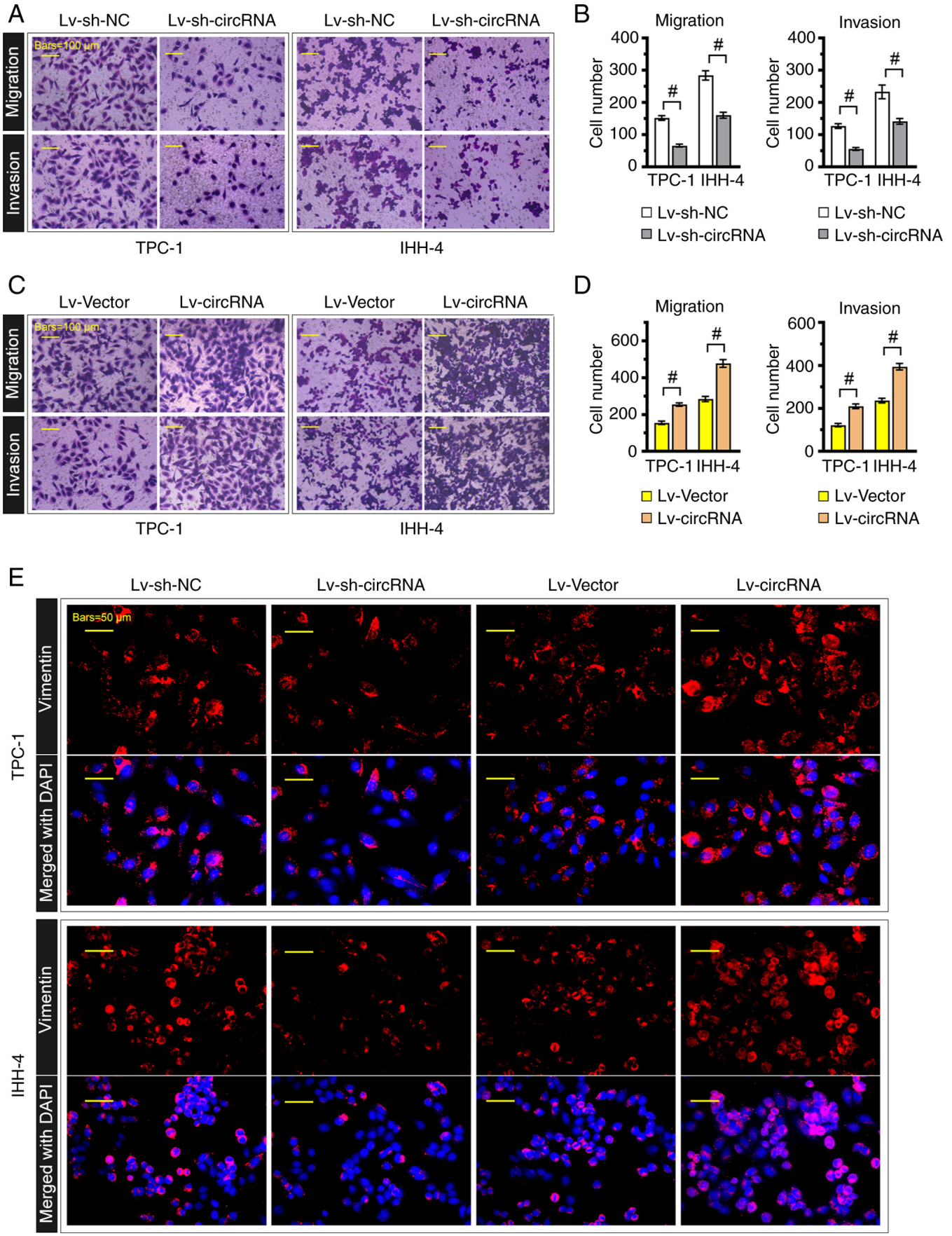

Figure 3. hsa_circ_0004846 promotes papillary thyroid carcinoma cell migration and invasion. (A) Transwell assays were performed to assess cell migration and invasion after hsa_circ_0004846 knockdown. (B) Histograms show the quantitative results of the Transwell assays. (C) Transwell assays were performed to assess cell migration and invasion after hsa_circ_0004846 overexpression. (D) Histograms show the quantitative results of the Transwell assays. (E) Immunofluorescence staining of vimentin in hsa_circ_0004846-overexpressing or -depleted TPC-1 and IHH-4 cells. $^{\#}P<0.05$. circ, circular; Lv, lentivirus; NC, negative control; sh, short hairpin.

overexpression significantly inhibited PELI1 expression (Fig. 5F). Considering that circRNAs often act as ceRNAs of miRNAs to regulate the expression of their target genes, these results indicated that hsa_circ_0004846 could promote PELI1 expression by inhibiting miR-142-3p expression.

PELI1 silencing reverses the cancer-promoting effects of hsa_circ_0004846. Since the molecular mechanism of hsa_circ_0004846 in the miR-142-3p/PELI1 axis was uncovered, a PELI1-silenced TPC-1 cell line was constructed to further explore the role of this axis in regulating tumorigenesis. The efficiency of cell transfection with PELI1-siRNA was verified by RT-qPCR analysis (Fig. 6A). Furthermore, the CCK-8 assay demonstrated that PELI1 silencing significantly inhibited cell viability in hsa_circ_0004846-overexpressing cells (Fig. 6B). Consistently, PELI1 silencing also reversed the enhanced invasion and migration of hsa_circ_0004846-overexpressing TPC-1 cells (Fig. 6C). In addition, western blotting revealed that the increased expression levels of p-AKT and p-GSK-3β induced by hsa_circ_0004846 were reversed after PELI1 knockdown (Fig. 6D).

Discussion

Currently, surgery and iodine 131 radiation therapy are the most common treatment strategies for PTC (22). According to the American Thyroid Association guidelines, prophylactic lymph node dissection is encouraged for high-risk patients with advanced primary tumors (23); however, the range of lymph node dissection and its auxiliary role in postoperative radioactive iodine are still a subject of controversy, as it is beneficial for preventing further recurrence, but is associated with a higher incidence of complications (22,24). Therefore, more effective treatment strategies are needed for patients with advanced and iodine-resistant PTC.

circRNA-related disorders have been well proven in several human diseases, including cancer (25,26). Emerging evidence has indicated that dysregulated circRNAs are associated with PTC progression. For example, circ_0011373 has been shown to be upregulated in PTC tissues and to promote PTC cell proliferation via the miR-1271/low-density lipoprotein receptor-related protein 6 axis (27). Jiang *et al* (28) suggested that circLDLR knockdown could induce PTC cell apoptosis via the miR-637/LIM domain only 4 axis. These findings indicated the role of circRNAs in PTC progression. To the best of our knowledge, the present study is the first to demonstrate that hsa_circ_0004846 is significantly upregulated in PTC tissues and cell lines. Notably, hsa_circ_0004846 is produced by reverse cleavage of the exon 3 of SAMD4A. To date, the expression and function of hsa_circ_0004846 have only been reported in osteosarcoma. Zhao *et al* (11) indicated that the high expression of hsa_circ_0004846 was associated with the metastasis and low overall survival rate of osteosarcoma cells. Their functional experiments also showed that hsa_circ_0004846 enhanced the malignant phenotypes of osteosarcoma cells *in vivo* and *vitro*. In the present study, the *in vitro* cell experiments revealed that hsa_circ_0004846 overexpression could markedly upregulate vimentin. A previous study has shown that vimentin is involved in cell attachment and migration in several types of cancer, including PTC (29).

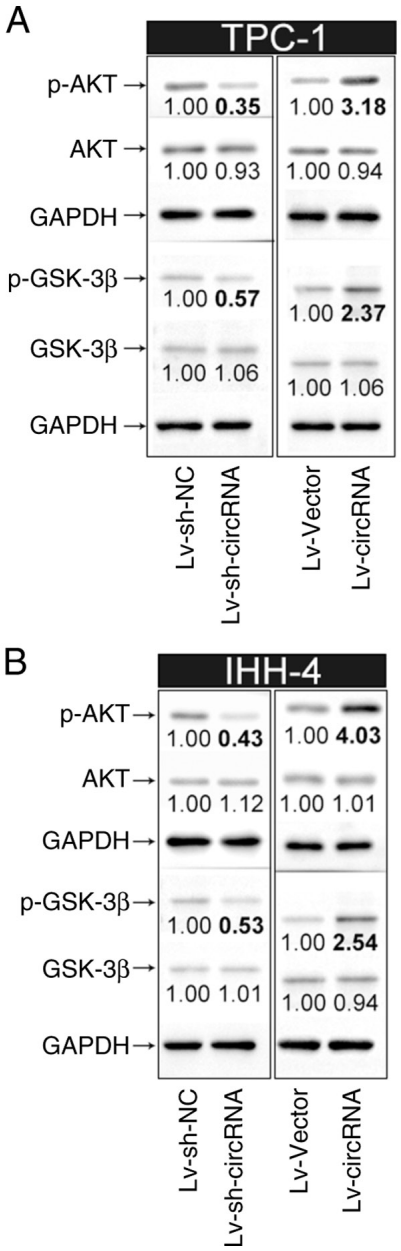

Figure 4. Effects of hsa_circ_0004846 on the PI3K/AKT pathway. Protein expression levels of p-AKT, AKT, p-GSK-3β and GSK-3β in (A) TPC-1 and (B) IHH-4 cells were detected by western blot analysis, GAPDH served as the internal control. circ, circular; Lv, lentivirus; NC, negative control; GSK-3β, glycogen synthase kinase-3β; p, phosphorylated; sh, short hairpin.

Furthermore, herein, hsa_circ_0004846 could activate the PI3K/AKT pathway, as evidenced by the increased expression levels of p-AKT and p-GSK-3β in hsa_circ_0004846-overexpressing PTC cells. GSK-3β, a major member of the destruction complex (APC, GSK-3β and Axin-2), is an important substrate of the PI3K/AKT pathway (30). In addition, the phosphorylation of AKT could promote the phosphorylation of GSK-3β to promote cancer cell metastasis (31). These findings indicated that hsa_circ_0004846 may serve an important role in the proliferation, migration and invasion of PTC cells.

Mechanistically, circRNAs have been widely reported to act as 'miRNA sponges' that can regulate the expression levels of miRNAs. In the current study, bioinformatics analysis using an online database (circRNA Interactome)

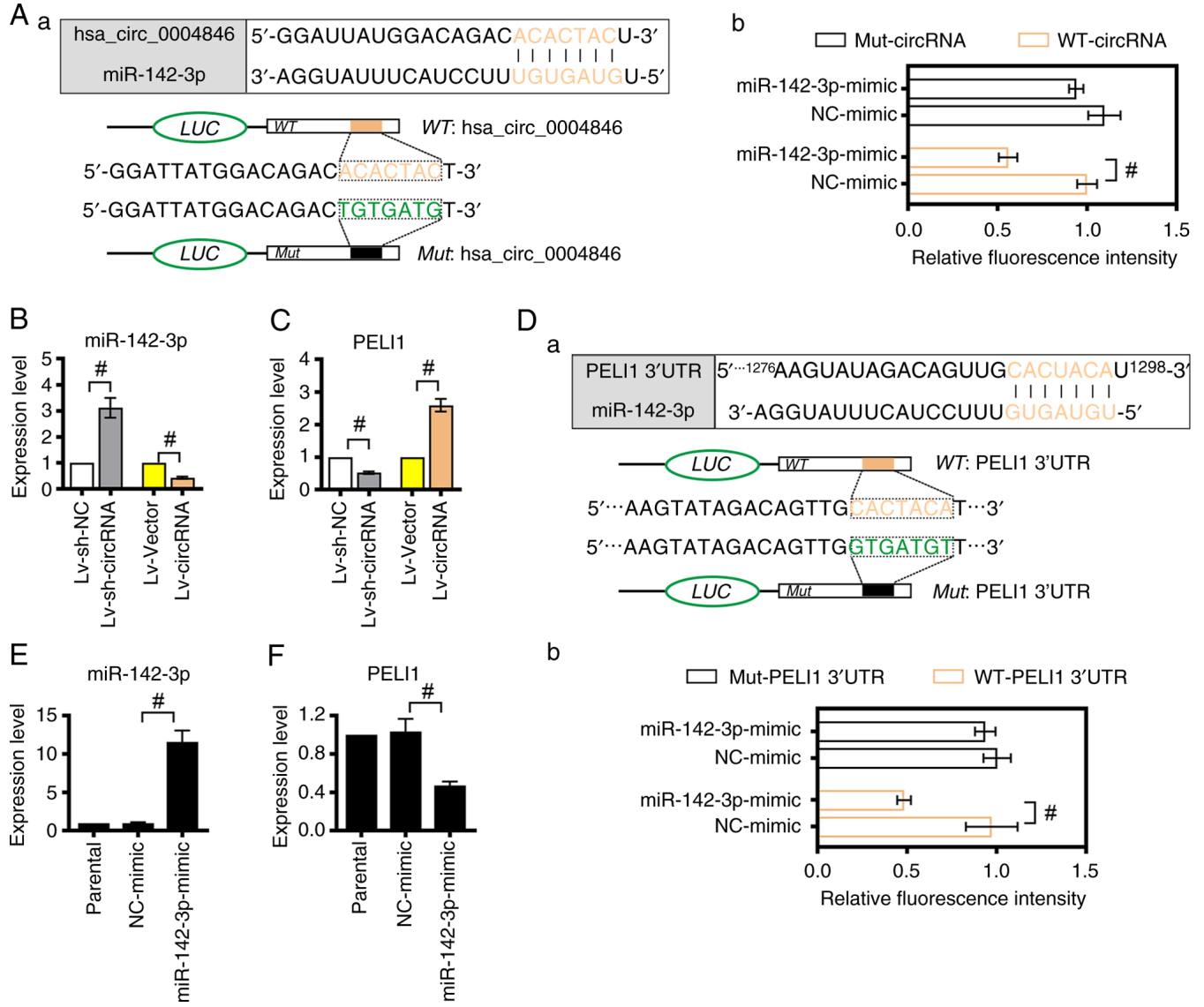

Figure 5. hsa_circ_0004846 upregulates PELI1 by sponging miR-142-3p. (A-a) Schematic diagram shows the binding site of miR-142-3p on hsa_circ_0004846 (https://circinteractome.nia.nih.gov/). (A-b) A dual-luciferase reporter assay was performed to verify the interaction between miR-142-3p and hsa_circ_0004846. Expression levels of (B) miR-142-3p and (C) PELI1 in hsa_circ_0004846-overexpressing or -depleted TPC-1 cells were detected by RT-qPCR. (D-a) Schematic diagram shows the binding site between miR-142-3p and the 3'UTR of PELI1, which was predicted using the miRDB online database (http://www.mirdb.org/). (D-b) A dual-luciferase reporter assay was carried out to verify the interaction between miR-142-3p and 3'-UTR PELI1. Expression levels of (E) miR-142-3p and (F) PELI1 in TPC-1 cells transfected with miR-142-3p-mimic or NC-mimic were measured by RT-qPCR analysis. #P<0.05. circ, circular; PELI1, Pellino E3 ubiquitin protein ligase 1; Lv, lentivirus; miR, microRNA; Mut, mutant; NC, negative control; RT-qPCR, reverse transcription-quantitative PCR; sh, short hairpin; WT, wild-type; 3'UTR, 3' untranslated region.

predicted that miR-142-3p may be a downstream factor of hsa_circ_0004846. This hypothesis was further verified by a dual-luciferase reporter assay. Previous studies have verified that miR-142-3p expression is reduced in follicular thyroid adenoma tissues, while the forced expression of miR-142-3p could suppress thyroid cancer WRO and FTC133 cell proliferation, thus supporting the tumor suppressor role of miR-142-3p in thyroid cancer (32). In the present study, miR-142-3p was revealed to be downregulated in hsa_circ_0004846-overexpressing PTC cells. In addition, miRNAs primarily act as the fine-tuners of target genes by binding to their 3'UTR (33). Based on the preliminary bioinformatics analysis results (miRDB), it was hypothesized that miR-142-3p might serve a role in regulating PELI1 expression. PELI1 is a novel cancer-related E3 ubiquitin ligase, which is involved in the progression of breast cancer (34), lung cancer (35) and lymphoma (36). Thus far, to the best of our knowledge, there are no studies reporting the association between miR-142-3p and PELI1. The current study was therefore the first to verify that miR-142-3p could bind to the 3'UTR of PELI1 and inversely regulate PELI1 mRNA abundance in PTC cells. Taken together, these results suggested that hsa_circ_0004846 could sponge miR-142-3p to regulate PELI1 expression.

Although the majority of studies have shown that PELI1 is a carcinogenic gene (37,38), a previous study revealed that PELI1 may act as a tumor suppressor gene in esophageal squamous cancer (ESC), since PELI1 overexpression could promote the radiotherapy sensitivity of ESC cells by inhibiting the non-canonical nuclear factor κB pathway (39). However,

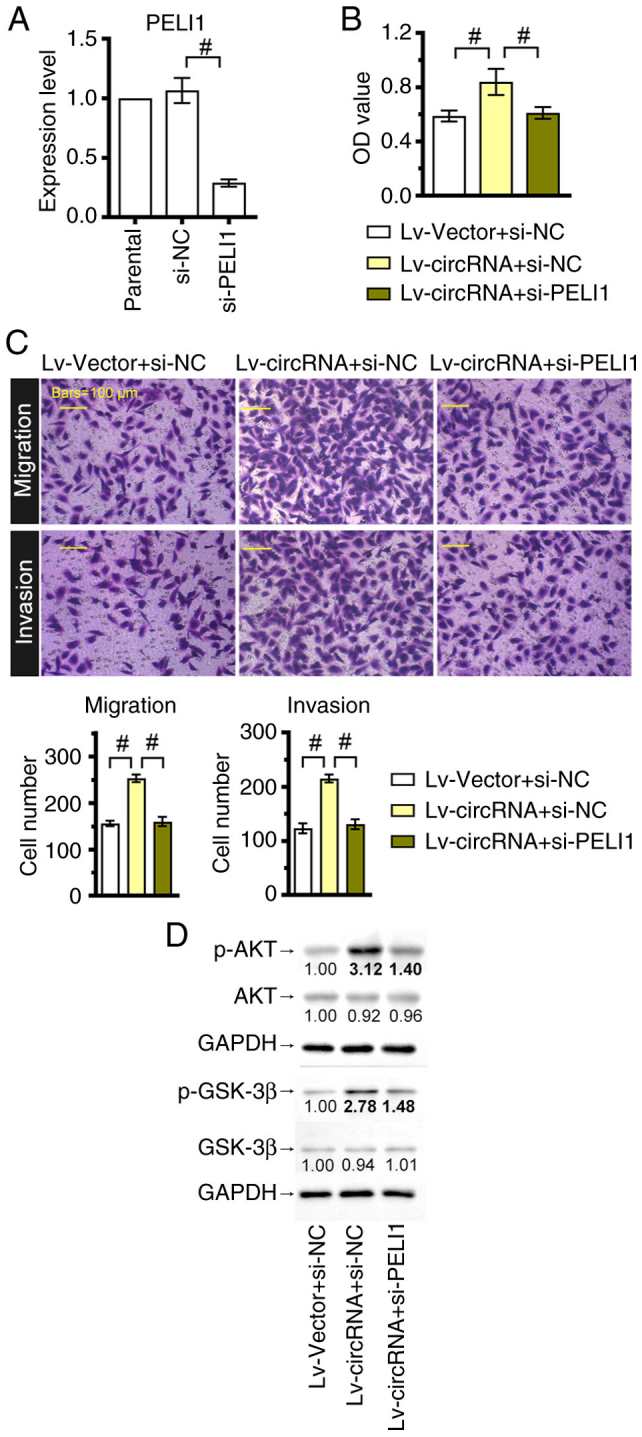

Figure 6. PELI1 mediates the effects of hsa_circ_0004846 on the malignant behavior of TPC-1 cells. (A) Reverse transcription-quantitative PCR was performed to detect the expression levels of PELI1 in TPC-1 cells transfected with si-PELI1 or si-NC. (B) Cell Counting Kit 8 and (C) Transwell assays were carried out to evaluate the viability, migration and invasion of TPC-1 cells. (D) Protein expression levels of p-AKT, AKT, p-GSK-3β and GSK-3β in TPC-1 cells were detected by western blot analysis. GAPDH was used as the internal control. #P<0.05. GSK-3β, glycogen synthase kinase-3β; Lv, lentivirus; NC, negative control; p, phosphorylated; PELI1, Pellino E3 ubiquitin protein ligase 1; si, small interfering.

Zheng *et al* (40) proposed that PELI1 was upregulated in PTC tissues, and PELI1 overexpression could promote the diffusion and migration of PTC cells by activating the PI3K/AKT pathway. In line with the aforementioned findings, the results of the present study indicated that PELI1 silencing could reverse activation of the PI3K/AKT pathway mediated by hsa_circ_0004846, thus suggesting that PELI1 could mediate the cancer-promoting effects of hsa_circ_0004846 on PTC cells.

There are some limitations in the present study. This work did not exclude the fact that other miRNAs could be involved in the regulation of PELI1 by hsa_circ_0004846, since a downstream target gene could be simultaneously targeted by several miRNAs. Therefore, this could be a focus of our future research. Furthermore, since the current study primarily focused on *in vitro* experiments, *in vivo* validation experiments should be performed in future studies.

In conclusion, the present study suggested that hsa_circ_0004846 overexpression promoted PTC cell proliferation, migration and invasion by activating the PI3K/AKT pathway. Mechanistically, hsa_circ_0004846 acted as a sponge of miR-142-3p to upregulate PELI1. Overall, the aforementioned findings indicated that hsa_circ_0004846 could serve a carcinogenic role in PTC by regulating the miR-142-3p/PELI1 axis.

Acknowledgements

Not applicable.

Funding

No funding was received.

Availability of data and materials

The data generated in the present study may be requested from the corresponding author.

Authors' contributions

XD and YW conceptualized and designed the study. XD, RL and JX performed the experiments. JX, GH, WW and QL contributed to data acquisition. XD, RL and YW analyzed the data. XD, RL, JX, GH, WW and QL interpreted the data. XD and RL confirm the authenticity of all the raw data. XD edited the original draft. XD and YW reviewed and edited the manuscript. All authors read and approved the final version of the manuscript.

Ethics approval and consent to participate

The present study was approved by the Ethics Committee of The First Affiliated Hospital of Anhui Medical University (approval no. Quick-PJ 2023-01-27) and was in accordance with the ethical standards formulated in The Declaration of Helsinki. All patients provided written informed.

Patient consent for publication

Not applicable.

Competing interests

The authors declare that they have no competing interests.

References

1. Gambardella C, Offi C, Clarizia G, Romano RM, Cozzolino I, Montella M, Di Crescenzo RM, Mascolo M, Cangiano A, Di Martino S, *et al*: Medullary thyroid carcinoma with double negative calcitonin and CEA: A case report and update of literature review. BMC Endocr Disord 19: 103, 2019.
2. Jiang C, Cheng T, Zheng X, Hong S, Liu S, Liu J, Wang J and Wang S: Clinical behaviors of rare variants of papillary thyroid carcinoma are associated with survival: A population-level analysis. Cancer Manag Res 10: 465-472, 2018.
3. Fröhlich E and Wahl R: The current role of targeted therapies to induce radioiodine uptake in thyroid cancer. Cancer Treat Rev 40: 665-674, 2014.
4. Ryu YJ, Lim SY, Na YM, Park MH, Kwon SY and Lee JS: Prostate-specific membrane antigen expression predicts recurrence of papillary thyroid carcinoma after total thyroidectomy. BMC Cancer 22: 1278, 2022.
5. Ashwal-Fluss R, Meyer M, Pamudurti NR, Ivanov A, Bartok O, Hanan M, Evantal N, Memczak S, Rajewsky N and Kadener S: circRNA biogenesis competes with pre-mRNA splicing. Mol Cell 56: 55-66, 2014.
6. Lei M, Zheng G, Ning Q, Zheng J and Dong D: Translation and functional roles of circular RNAs in human cancer. Mol Cancer 19: 30, 2020.
7. Zhang Q, Wang W, Zhou Q, Chen C, Yuan W, Liu J, Li X and Sun Z: Roles of circRNAs in the tumour microenvironment. Mol Cancer 19: 14, 2020.
8. Zhang D, Tao L, Xu N, Lu X, Wang J, He G, Tang Q, Huang K, Shen S and Chu J: CircRNA circTIAM1 promotes papillary thyroid cancer progression through the miR-646/HNRNPA1 signaling pathway. Cell Death Discov 8: 21, 2022.
9. Bi W, Huang J, Nie C, Liu B, He G, Han J, Pang R, Ding Z, Xu J and Zhang J: CircRNA circRNA_102171 promotes papillary thyroid cancer progression through modulating CTNNBIP1-dependent activation of β-catenin pathway. J Exp Clin Cancer Res 37: 275, 2018.
10. Wei W, Ji L, Duan W and Zhu J: CircSAMD4A contributes to cell doxorubicin resistance in osteosarcoma by regulating the miR-218-5p/KLF8 axis. Open Life Sci 15: 848-859, 2020.
11. Zhao Y and Zhang J: CircSAMD4A accelerates cell proliferation of osteosarcoma by sponging miR-1244 and regulating MDM2 mRNA expression. Biochem Biophys Res Commun 516: 102-111, 2019.
12. Xie C, Chen B, Wu B, Guo J, Shi Y and Cao Y: CircSAMD4A regulates cell progression and epithelial-mesenchymal transition by sponging miR-342-3p via the regulation of FZD7 expression in osteosarcoma. Int J Mol Med 46: 107-118, 2020.
13. Zhong Y, Du Y, Yang X, Mo Y, Fan C, Xiong F, Ren D, Ye X, Li C, Wang Y, *et al*: Circular RNAs function as ceRNAs to regulate and control human cancer progression. Mol Cancer 17: 79, 2018.
14. Lee YS and Dutta A: MicroRNAs in cancer. Annu Rev Pathol 4: 199-227, 2009.
15. White WL: Erratum to: Why I hate the index finger. Hand (N Y) 6: 233, 2011.
16. Chen Y, Dong B, Huang L and Huang H: Serum microRNAs as biomarkers for the diagnosis of papillary thyroid carcinoma: A meta-analysis. Bosn J Basic Med Sci 22: 862-871, 2022.
17. Jiang Y, Liu Y, Zhang Y, Ouyang J, Feng Y, Li S, Wang J, Zhang C, Tan L, Zhong J and Zou L: MicroRNA-142-3P suppresses the progression of papillary thyroid carcinoma by targeting FN1 and inactivating FAK/ERK/PI3K signaling. Cell Signal 109: 110792, 2023.
18. Almeida JL and Korch CT: Authentication of human and mouse cell lines by short tandem repeat (STR. DNA genotype analysis. In Assay Guidance Manual, Markossian S, Grossman A, Arkin M, Auld D, Austin C, Baell J, Brimacombe K, Chung TDY, Coussens NP, Dahlin JL, *et al*. (eds.). Eli Lilly & Company and the National Center for Advancing Translational Sciences, 2004.
19. Livak KJ and Schmittgen TD: Analysis of relative gene expression data using real-time quantitative PCR and the 2(-Delta Delta C(T). method. Methods 25: 402-408, 2001.
20. Zhao X, Fu J, Hu B, Chen L, Wang J, Fang J, Ge C, Lin H, Pan K, Fu L, *et al*: Serine metabolism regulates YAP activity through USP7 in colon cancer. Front Cell Dev Biol 9: 639111, 2021.
21. Petrulea MS, Plantinga TS, Smit JW, Georgescu CE and Netea-Maier RT: PI3K/Akt/mTOR: A promising therapeutic target for non-medullary thyroid carcinoma. Cancer Treat Rev 41: 707-713, 2015.
22. Conzo G, Mauriello C, Docimo G, Gambardella C, Thomas G, Cavallo F, Tartaglia E, Napolitano S, Varriale R, Rossetti G, *et al*: Clinicopathological pattern of lymph node recurrence of papillary thyroid cancer. Implications for surgery. Int J Surg 12 (Suppl 1): S194-S197, 2014.
23. Cooper DS, Doherty GM, Haugen BR, Kloos RT, Lee SL, Mandel SJ, Mazzaferri EL, McIver B, Pacini F, Schlumberger M, *et al*: Revised American Thyroid Association management guidelines for patients with thyroid nodules and differentiated thyroid cancer. Thyroid 19: 1167-1214, 2009.
24. Conzo G, Docimo G, Mauriello C, Gambardella C, Esposito D, Cavallo F, Tartaglia E, Napolitano S and Santini L: The current status of lymph node dissection in the treatment of papillary thyroid cancer. A literature review. Clin Ter 164: e343-e346, 2013.
25. Wang L, Wang P, Su X and Zhao B: Circ_0001658 promotes the proliferation and metastasis of osteosarcoma cells via regulating miR-382-5p/YB-1 axis. Cell Biochem Funct 38: 77-86, 2020.
26. Ding B, Fan W and Lou W: hsa_circ_0001955 Enhances in vitro proliferation, migration, and invasion of HCC cells through miR-145-5p/NRAS axis. Mol Ther Nucleic Acids 22: 445-455, 2020.
27. Huang G, Mao L and Hu X: Circ_0011373 promotes papillary thyroid carcinoma progression by regulating miR-1271/LRP6 axis. Hormones (Athens) 22: 375-387, 2023.
28. Jiang YM, Liu W, Jiang L and Chang H: CircLDLR promotes papillary thyroid carcinoma tumorigenicity by regulating miR-637/LMO4 axis. Dis Markers 2021, 3977189, 2021.
29. Chong ST, Tan KM, Kok CYL, Guan SP, Lai SH, Lim C, Hu J, Sturgis C, Eng C, Lam PYP and Ngeow J: IL13RA2 is differentially regulated in papillary thyroid carcinoma vs follicular thyroid carcinoma. J Clin Endocrinol Metab 104: 5573-5584, 2019.
30. Jere SW, Houreld NN and Abrahamse H: Role of the PI3K/AKT mTOR and GSK3β. signalling pathway and photobiomodulation in diabetic wound healing. Cytokine Growth Factor Rev 50: 52-59, 2019.
31. Han J, Zhang M, Nie C, Jia J, Wang F, Yu J, Bi W, Liu B, Sheng R, He G, *et al*: miR-215 suppresses papillary thyroid cancer proliferation, migration, and invasion through the AKT/GSK-3β/Snail signaling by targeting ARFGEF1. Cell Death Dis 10: 195, 2019.
32. Colamaio M, Puca F, Ragozzino E, Gemei M, Decaussin-Petrucci M, Aiello C, Bastos AU, Federico A, Chiappetta G, Del Vecchio L, *et al*: miR-142-3p down-regulation contributes to thyroid follicular tumorigenesis by targeting ASH1L and MLL1. J Clin Endocrinol Metab 100: E59-E69, 2015.
33. Bartel DP: MicroRNAs: Target recognition and regulatory functions. Cell 136: 215-233, 2009.
34. Liu SS, Qi J, Teng ZD, Tian FT, Lv XX, Li K, Song YJ, Xie WD, Hu ZW and Li X: Resistomycin attenuates triple-negative breast cancer progression by inhibiting E3 ligase Pellino-1 and inducing SNAIL/SLUG degradation. Signal Transduct Target Ther 5: 133, 2020.
35. Jeon YK, Kim CK, Hwang KR, Park HY, Koh J, Chung DH, Lee CW and Ha GH: Pellino-1 promotes lung carcinogenesis via the stabilization of Slug and Snail through K63-mediated polyubiquitination. Cell Death Differ 24: 469-480, 2017.
36. Park HY, Go H, Song HR, Kim S, Ha GH, Jeon YK, Kim JE, Lee H, Cho H, Kang HC, *et al*: Pellino 1 promotes lymphomagenesis by deregulating BCL6 polyubiquitination. J Clin Invest 124: 4976-4988, 2014.
37. Fei X, Zhu C, Liu P, Liu S, Ren L, Lu R, Hou J, Gao Y, Wang X and Pan Y: PELI1: Key players in the oncogenic characteristics of pancreatic Cancer. J Exp Clin Cancer Res 43: 91, 2024.
38. Zhou W, Hu Y, Wang B, Yuan L, Ma J and Meng X: Aberrant expression of PELI1 caused by Jagged1 accelerates the malignant phenotype of pancreatic cancer. Cell Signal 111: 110877, 2023.
39. Ko CJ, Zhang L, Jie Z, Zhu L, Zhou X, Xie X, Gao T, Yang JY, Cheng X and Sun SC: The E3 ubiquitin ligase Peli1 regulates the metabolic actions of mTORC1 to suppress antitumor T cell responses. EMBO J 40: e104532, 2021.
40. Zheng T, Zhou Y, Xu X, Qi X, Liu J, Pu Y, Zhang S, Gao X, Luo X, Li M, *et al*: MiR-30c-5p loss-induced PELI1 accumulation regulates cell proliferation and migration via activating PI3K/AKT pathway in papillary thyroid carcinoma. J Transl Med 20: 20, 2022.